



Impact of different surfactants and ultrasonication time on the stability and thermophysical properties of hybrid nanofluids

Hong Wei Xian^a, Nor Azwadi Che Sidik^{a,*}, R. Saidur^{b,c}

^a Malaysia – Japan International Institute of Technology (MJIT), Universiti Teknologi Malaysia Kuala Lumpur, Jalan Sultan Yahya Petra (Jalan Semarak), 54100 Kuala Lumpur, Malaysia

^b Research Centre for Nano-Materials and Energy Technology (RCNMET), School of Science and Technology, Sunway University, No. 5, Jalan Universiti, Bandar Sunway, 47500 Petaling Jaya, Selangor, Malaysia

^c Department of Engineering, Lancaster University, LA1 4YW, United Kingdom

ARTICLE INFO

Keywords:

Graphene nanoplatelets
Hybrid nanofluid
Thermophysical properties
Surfactant

ABSTRACT

Graphene based nanofluids are getting more attention among researchers due to their exceptional thermal conductivity. In the present study, stable hybrid nanofluids were produced by dispersing graphene nanoplatelets (GnPs) and titanium dioxide (TiO₂) in a mixture of distilled water and ethylene glycol (DW/EG) using a two-step method. For comparison purpose, GnPs were dispersed into the same base fluid and labelled as mono nanofluid. The impact of different surfactants and sonication time on nanofluids' stability was determined by sedimentation method, zeta potential analysis, and absorbency test. It was observed that the addition of hexadecyltrimethylammonium bromide (CTAB) showed the highest degree of stability in all analyses, with minimal sedimentation up to 40 days. Thermophysical properties of nanofluids with CTAB were measured from 30 °C to 70 °C at 0.1, 0.075, 0.05, and 0.025 wt% concentrations of nanoparticles. The maximum thermal conductivity enhancement of base fluid was found to be 23.74% when 0.1 wt% of COOH-GnP was added at 60 °C. Hybrid nanofluid showed higher thermal conductivity than mono nanofluid at all concentration and temperature ranged from 30 to 50 °C. Both mono and hybrid nanofluids showed Newtonian behaviour in which shear stress increased linearly with increasing shear rate. Mono nanofluid with 0.1 wt% concentration showed the highest viscosity at 40 °C, which was 32.54% and 4.85% higher than base fluid and 0.1 wt% hybrid nanofluid, respectively. The enhanced properties of this hybrid nanofluid could be used as an alternate heat transfer medium in an automobile cooling system.

1. Introduction

Nanotechnology is infiltrating human lives worldwide yet the public may not be aware of it. Electronic gadget processors nowadays are equipped with 10 nm of transistors, which promote less power consumption and higher performance. In the past few decades, researchers have examined the performance of this leading technology in diverse applications: biomedical, heat exchangers, photocatalysts, photovoltaic and others. However, one of the largest demands in the industry is the need of a highly efficient heat rejection mechanism to increase the overall efficiency of a working system. Generally, there are two methods to improve cooling efficiency: passive cooling and active cooling. The former technique is about modifying the design to control fluid flow behaviour, whereas the latter method involves the use of an external device or fluid to remove excess heat. In 1995, Choi and Eastman [1] innovated a novel heat transfer fluid called nanofluid. It is a suspension consisting of nanoscale solid particles and conventional

base fluid. These tiny particles are composed of high thermal conductivity and their large surface-to-volume ratio can even enhance the heat exchange interaction between solid and fluid particles. At the beginning, many researchers reported on the significant improvement of thermal properties when nanoparticles were added into base fluid, which included metals, metal oxides, and non-metals in both organic and inorganic solvents. Due to the incessant pursue of nanofluid with more desirable behaviour, hybrid nanofluid was first examined by Jana et al. [2] in 2007. Hybrid nanofluid was said to exhibit combined properties of different nanoparticles due to the synergistic effect and hence, showed more enhancement than mono nanofluid in past studies [3–6] in most cases.

During these last few years, graphene has been gaining immense attention from researchers due to its superior thermal conductivity as compared to other materials. Graphene is a monolayer exfoliated from graphite (one-atom-thick) with sp²-bonded carbon atoms in hexagonal array. It is a two-dimensional structure and looks like a planar form of

* Corresponding author.

Nomenclature

Abbreviations

2D	Two-dimensional
A	Absorbency
ASHRAE	American Society of Heating, Refrigeration and Air-Conditioning Engineer
C	Concentration
COOH-GnP	Carboxyl-functionalized graphene nanoplatelets
DW	Distilled water
EG	Ethylene glycol
<i>I</i>	Transmitted light intensity
<i>I₀</i>	Initial light source intensity
<i>L</i>	Optical path length (cm)
MWCNT	Multi-walled carbon nanotubes

SWCNT	Single walled carbon nanotubes
TEM	Transmission electron microscopy
TiO ₂	Titanium oxide
wt%	Weightage concentration

Greek symbols

<i>E</i>	molar extinction coefficient
----------	------------------------------

Subscript

<i>O</i>	Initial
<i>Bf</i>	Base fluid
<i>Nf</i>	Nanofluid
<i>R</i>	Ratio

carbon nanotubes. Multi layers of graphene with platelet shape are known as graphene nanoplatelets (GnPs) and numerous past researches included GnPs as heat transfer fluid due to their remarkable heat transfer enhancement. Many researchers reported that the addition of GnP into various base fluids, such as water/ethylene glycol [7,8], water [9,10], and diesel oil [11], showed enhancement in thermal properties. In addition, mixing GnP with other carbon-based nanoparticles further enhanced thermal conductivity of base fluid even more than nanofluid with a single type of nanoparticles [12].

Although GnP-based nanofluids were reported to exhibit greater thermal conductivity in comparison to most nanofluids, they have poor stability of dispersing in polar solvents. The hydrophobic nature of GnP can be polarised by introducing covalent or non-covalent functionalisation for better dispersion. The former approach modifies the surface properties of GnP by chemical reactions; as a result, the intrinsic behaviour of GnP might be affected [13]. Several studies reported on treating GnP composites with acid [11,14] and alcohol [15] by attaching hydrophilic functional groups on GnP surface such as carboxyl and hydroxyl groups and eventually they obtained improved suspension stability. On the other hand, non-covalent functionalisation stabilises GnP by forming weak interactions (electrostatic, van der Waals or π - π) with target molecules due to the sp^2 network [16]. This method was involved in many past studies, which included the use of surfactants such as Triton X-100 [17], sodium dodecylbenzene sulfonate (SDBS) [18,19], gum Arabic [20], and sodium deoxycholate (SDC) [8] in GnP-based nanofluids. Nevertheless, the drawback of adding an extra compound in suspension indicates higher viscosity, which is non-ideal in liquid flowing applications (increased pressure drop) as an excessive amount of surfactants could affect the stability and thermal conductivity of nanofluids [21,22].

In this study, the authors were inclined to produce graphene-based hybrid nanofluid by direct mixing of two different powders using a two-step method. Several past studies employed this type of direct mixing method for hybrid nanofluids [12,23,24]. A review from Leong et al. [25] suggested that nanocomposite produced from multiple chemical and physical processes would eventually split away due to ultrasonication. Normally, past researchers synthesised graphene nanocomposite through a chemical reaction process, followed by dispersion into base fluid. They functionalised graphene and coated it with secondary nanoparticles such as platinum [26] and silver [14].

Based on the authors' best knowledge, there is no work reported on TiO₂-GnP dispersed nanofluid. Nevertheless, a few studies focused on the use of TiO₂-GnP nanocomposite as electrode in photocatalytic [27] and photovoltaic (dye-sensitised solar cells) [28] applications. Most of them reported on improved electrical conductivity and electrochemical sensitivity [29] of this nanocomposite. The purpose of this study is to measure thermal conductivity, viscosity, and stability of this novel

hybrid nanofluid. Different ultrasonication time and surfactants were compared in terms of suspension stability, followed by the measurement of aforementioned properties ranging from 30 °C to 70 °C with different nanoparticle weightage concentrations (Figs. 1 and 5).

2. Methodology

2.1. Preparation of nanofluid

Titanium oxide (TiO₂) nanopowder was purchased from US Research Nanomaterials, Inc. The TiO₂ powder had purity of 99.9%, bulk density of 3900 kg/m³, and diameter of 5 nm. For carboxyl-functionalised graphene nanoplatelets (COOH-GnPs), they were purchased from Cheap Tubes Inc. COOH-GnP was labelled with 99 wt% purity, grade 4, 2 μ m length, < 4 nm of thickness, and surface area of > 700 m²/g. Ethylene glycol (reagent grade) was purchased from R&M Chemicals.

A two-step method was employed to produce both mono and hybrid nanofluids. Firstly, distilled water and ethylene glycol (DW/EG) were mixed in a 60:40 weightage ratio as base fluid. Surfactant (1:1 concentration of nanoparticles) was added into DW/EG and stirred for 10 min. COOH-GnP powder was used to produce mono nanofluid in this study. For hybrid nanofluid, TiO₂ and COOH-GnP powder were mixed into DW/EG with a 50:50 weightage ratio using a magnetic stirrer (30 min, 500 rpm). Lastly, the mixture was sonicated again using a probe sonicator (FS-1200 N, frequency: 20 kHz, power output: 1200 W,



Fig. 1. Ultrasonication of nanofluid.

18 mm probe) at 60% amplitude to disperse nanoparticles from agglomerating. During the whole sonication process, sample temperature was maintained under 40 °C to prevent possible degradation of surfactant at high temperature.

2.2. Transmission electron microscope imaging

Morphology and size of nanoparticles were estimated by using a transmission electron microscope (TEM). Before inspection, a few drops of ethanol were mixed with nanopowder and the mixture was placed on a copper grid, followed by air drying.

2.3. Evaluation of nanofluid stability

The effects of different surfactants and ultrasonication time (15, 30, 60, and 90 min) were studied to obtain the optimum combination that produces nanofluid with high stability. Firstly, a visual sedimentation method was used to observe the forming of supernatant and sediment in nanofluid. This method can provide visible change over time; however, it lacks quantitative results to evaluate the degree of stability. Therefore, the stability of nanofluids was further determined in this study by using particle analyser (Anton Paar Litesizer 500) and ultraviolet-visible (UV-vis) spectrophotometer (Perkin Elmer Lambda 750). High concentration (0.5 and 1.0 wt%) of graphene-based suspensions caused significant noises in spectrum and its naturally black appearance tend to absorb most transmitted light from source. 0.1 wt% of graphene-based nanofluid was found to provide clearer results and hence this concentration was standardized for all stability evaluations in this study.

Even though six different surfactants were used in this study, only nanofluids with higher than ± 30 mV in zeta potential value were considered for UV-vis spectrophotometer long term stability inspection. Nanofluid with the highest stability and the least possible sonication time was selected for thermophysical properties measurement. The range of measurement covered from 30 °C to 70 °C and included four different concentrations (0.025, 0.05, 0.075, and 0.1 wt%).

2.4. Measurement of thermophysical properties

Thermal conductivity of nanofluids was measured by using Decagon KD2 Pro, which works via a transient hot wire method. In this study, KS1 sensor was used and it had an uncertainty of $\pm 5.0\%$. A water bath was used to achieve temperature equilibrium environment with an accuracy of 0.1 °C. A total of 15 readings with 5 min interval time were recorded for each sample, with the average value reported in a later section.

A rheometer (Anton Paar MCR92) with concentric cylinder (CC39) was used to measure low-viscosity liquid samples. The rheometer works

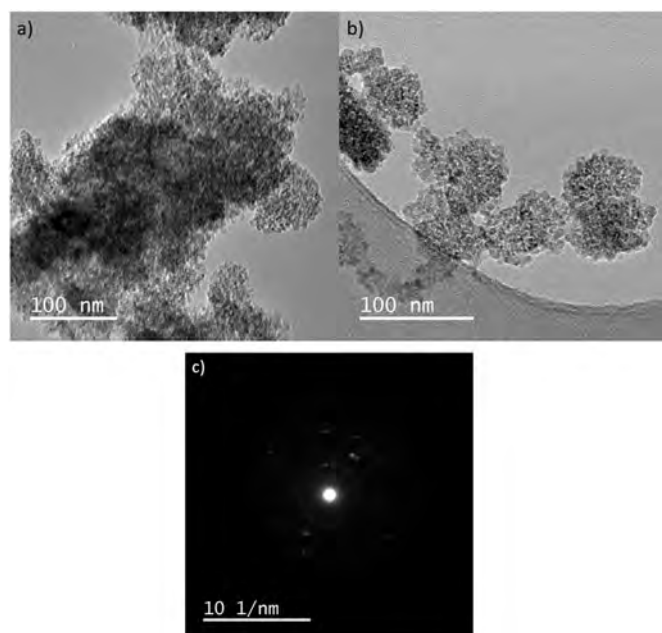


Fig. 3. TEM images of TiO₂ a) Before ultrasonication (50,000 × magnification), b) Before ultrasonication (50,000 × magnification), c) Selected area electron diffraction pattern.

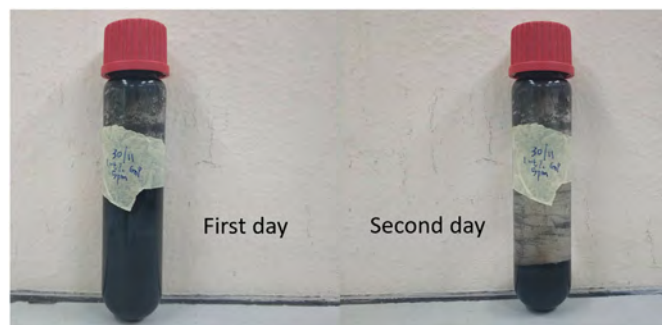


Fig. 4. Behavior of COOH-GnP in DW/EG.

according to DIN 53019 and ISO 3219 standards, which suggest measuring viscosity and flow curves using a rotational viscometer with defined shear rate. 60 ml of sample and 5 mm of gap were found to be optimum for obtaining accurate results. The flow behaviour of samples was determined at different shear rates and temperature.

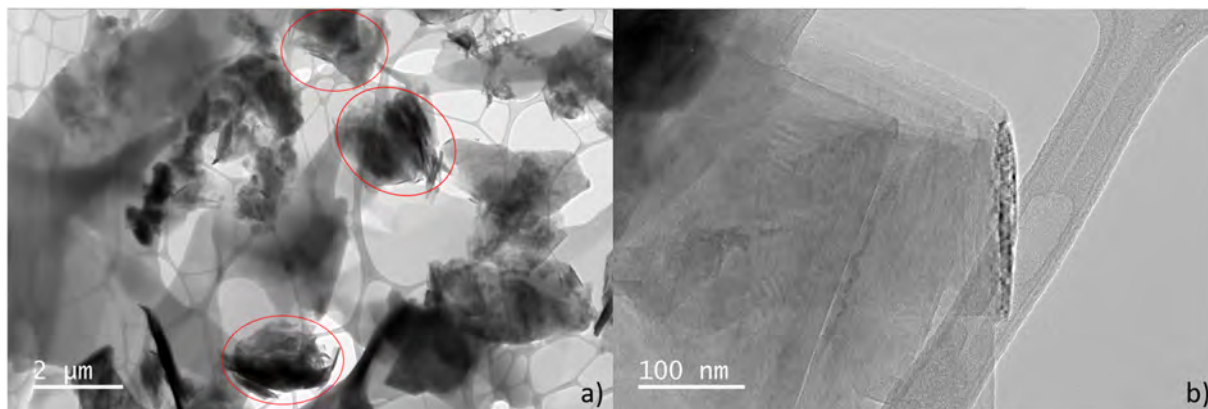


Fig. 2. TEM images of COOH-GnP a) 2000 × magnification and b) 50,000 × magnification.

3. Results and discussion

3.1. Characterisation

3.1.1. Morphology and particles size

TEM images of COOH-GnP and TiO₂ are shown in Figs. 2 and 3, respectively. Some flake-like structures can be noticed in Fig. 2a, and circled parts showed COOH-GnP length of about 2 μm. Fig. 2b shows limited graphene layers (3–4 layers) in COOH-GnP sheets, which was the same as the information provided by suppliers. Figs. 3a and b illustrate the differences of TiO₂ nanoparticles agglomeration before and after the ultrasonication process. Even with 15 min of ultrasonication, the agglomeration of TiO₂ nanoparticles was greatly reduced. In addition, TiO₂ nanoparticles were observed to be polycrystalline in Fig. 3c and the estimated particle size was about 5 to 7 nm.

3.1.2. Sedimentation method

The purchased COOH-GnP was insoluble in water; thus, it showed the hydrophobic behaviour in water-based mixture. Fig. 4 below shows poor dispersability of COOH-GnP in DW/EG. A non-covalent functionalisation approach was used to enhance the solubility of COOH-GnP without shattering its intrinsic properties. In this study, various surfactants were used to increase the stability of both mono (COOH-GnP) and hybrid (TiO₂-(COOH-GnP)) nanofluids by reducing fluid adhesion and providing steric repulsions to counteract the van der Waals attraction force. In later sections, mono and hybrid nanofluids are abbreviated as G and H, respectively.

3.1.3. Zeta potential analysis

Zeta potential means electrostatic repulsion force between nanoparticles and base fluid. High repulsion force indicates high stability of nanofluid, whereby |30 mV| is generally considered as a benchmark for a stable nanofluid and excellent nanofluid stability may exceed |60 mV| [30,31]. All samples for the zeta potential analysis were fixed at 0.1 wt % and the average of five readings was reported. As shown in Fig. 6, it is observed that ultrasonication duration did not significantly affect the initial stability of nanofluids in terms of zeta potential value, except for samples with Triton X-100. It was also found that SDBS matched the best with both COOH-GnP and TiO₂-(COOH-GnP) nanofluids, with about -52 mV to -60 mV for mono nanofluid and -42 mV to -46 mV for hybrid nanofluid. The result was similar to past research on graphene-water nanofluid, which reported a zeta potential value of -63.7 mV [32].

Referring back to the details of surfactants tabulated in Table 1, the resulting surface charge of nanofluids was expected as shown in Fig. 6. Anionic surfactants (SDC, SDS and SDBS) contributed to negatively charged suspension and a positive charged one was obtained by adding cationic surfactant (CTAB). For neutral surfactants (PVP and Triton X-100), mono nanofluids showed more negative value than hybrid nanofluid due to the negative surface charge of COOH-GnP. Neutral charged surfactant decreased the zeta potential of suspension due to its absorption on particle-liquid interface, while both cationic and anionic surfactants formed a diffused layer around nanoparticles and hence increased zeta potential magnitude [33]. The increment in stability was due to the coating of surfactant on nanoparticles, which provided a

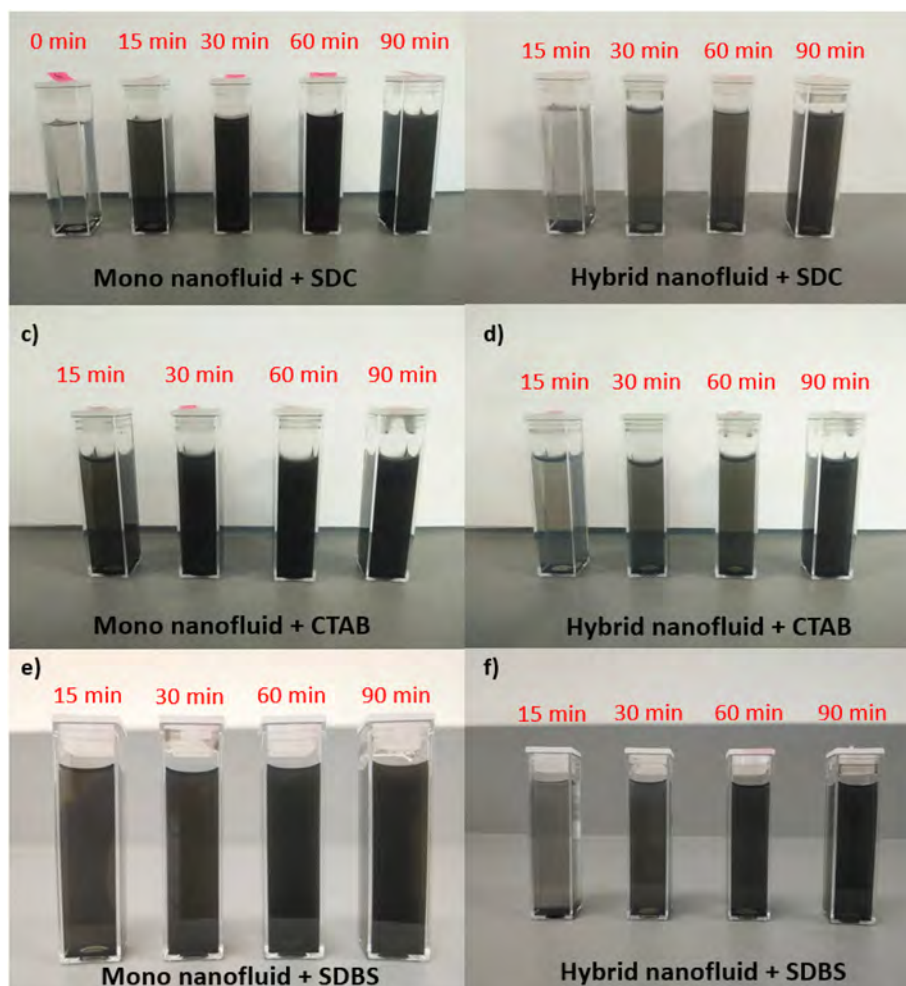


Fig. 5. Visual inspection of sedimentation of nanofluids with different surfactants and ultra-sonication time after 40 days.

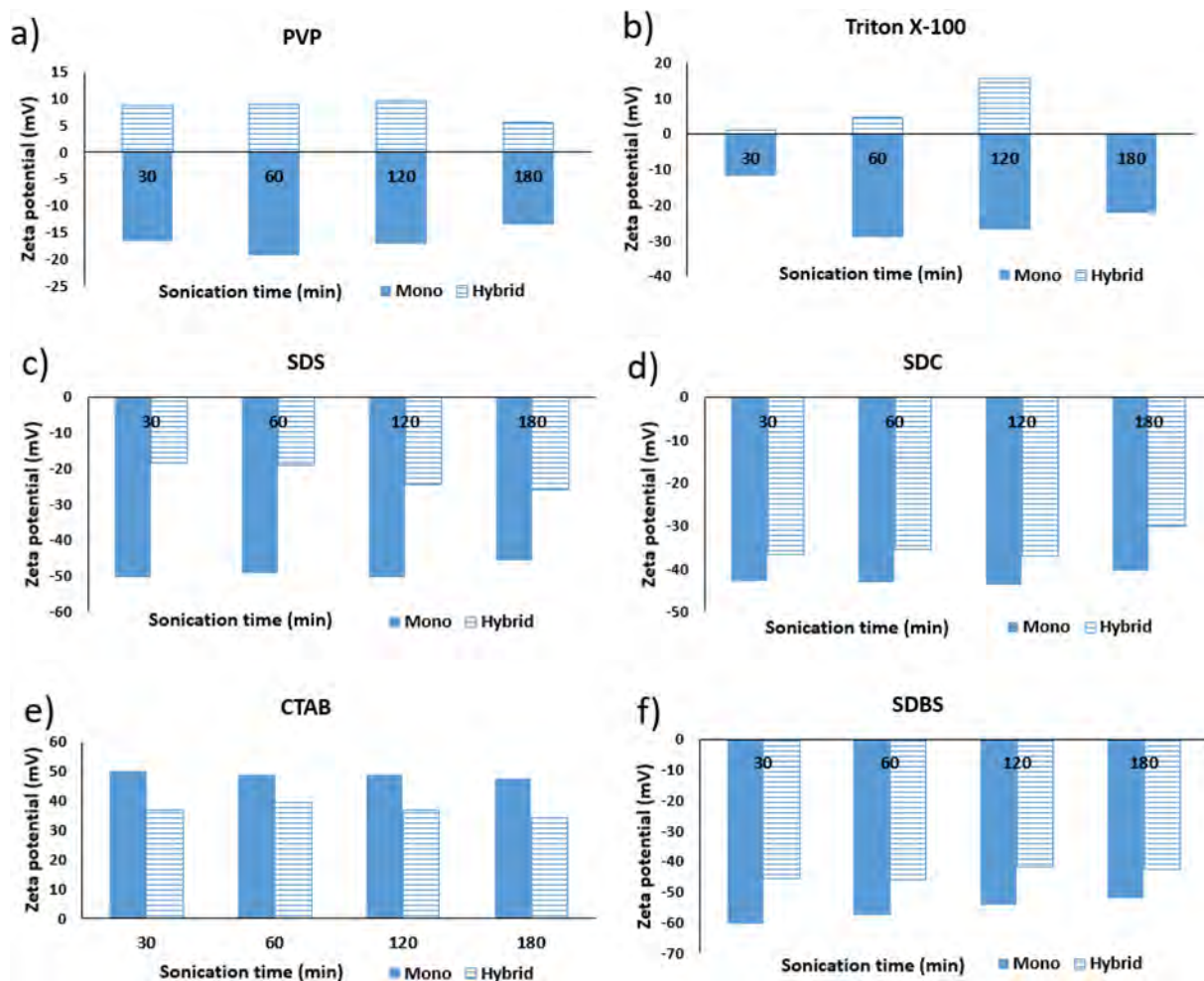


Fig. 6. Zeta potential of mono and hybrid nanofluid using different surfactant at various ultrasonic sonication duration. a) PVP b) Triton X-100 c) SDS d) SDC e) CTAB f) SDBS.

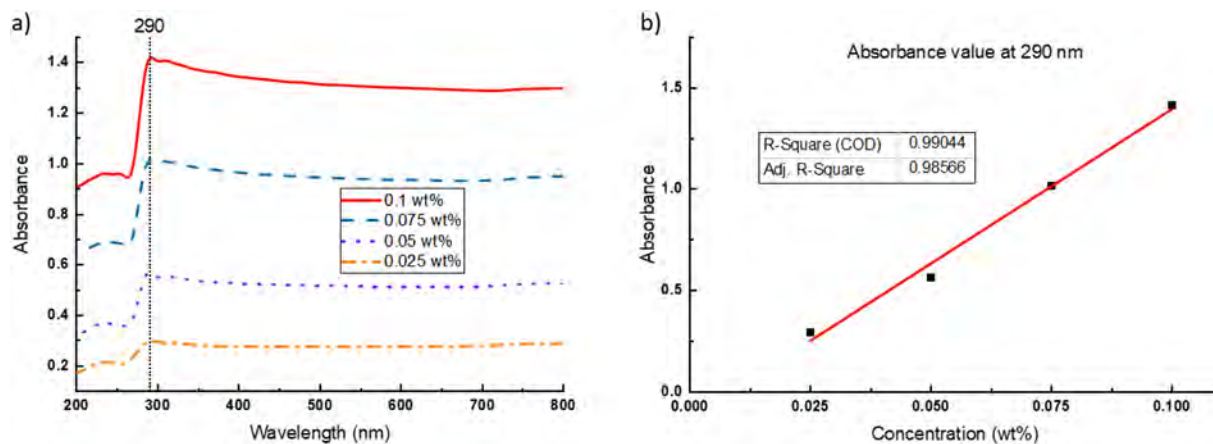


Fig. 7. a) Spectrum with peak absorbance, b) Absorbance against different concentrations.

dominating electrostatic repulsion over the van der Waals force and thus prevented nanoparticles from agglomerating. As indicated in Fig. 6, the use of ionic surfactants resulted in higher stability of nanofluids due to the fact that the electrostatic assembly process was more suitable for highly charged COOH-GnP used in the present study, whereas steric stabilisation from the use of non-ionic surfactant led to poor stability of nanofluids.

3.2. UV-vis spectroscopy analysis

As nanoparticles sedimented in nanofluid, the absorbance in supernatant part dropped with concentration. The relationship between these two variables is expressed as the Beer-Lambert law as in Eq. (1), where ϵ , c , l , I_0 and I indicate molar extinction coefficient, concentration, optical path length, initial light source intensity, and intensity after passing through the samples, respectively. This law proposes that

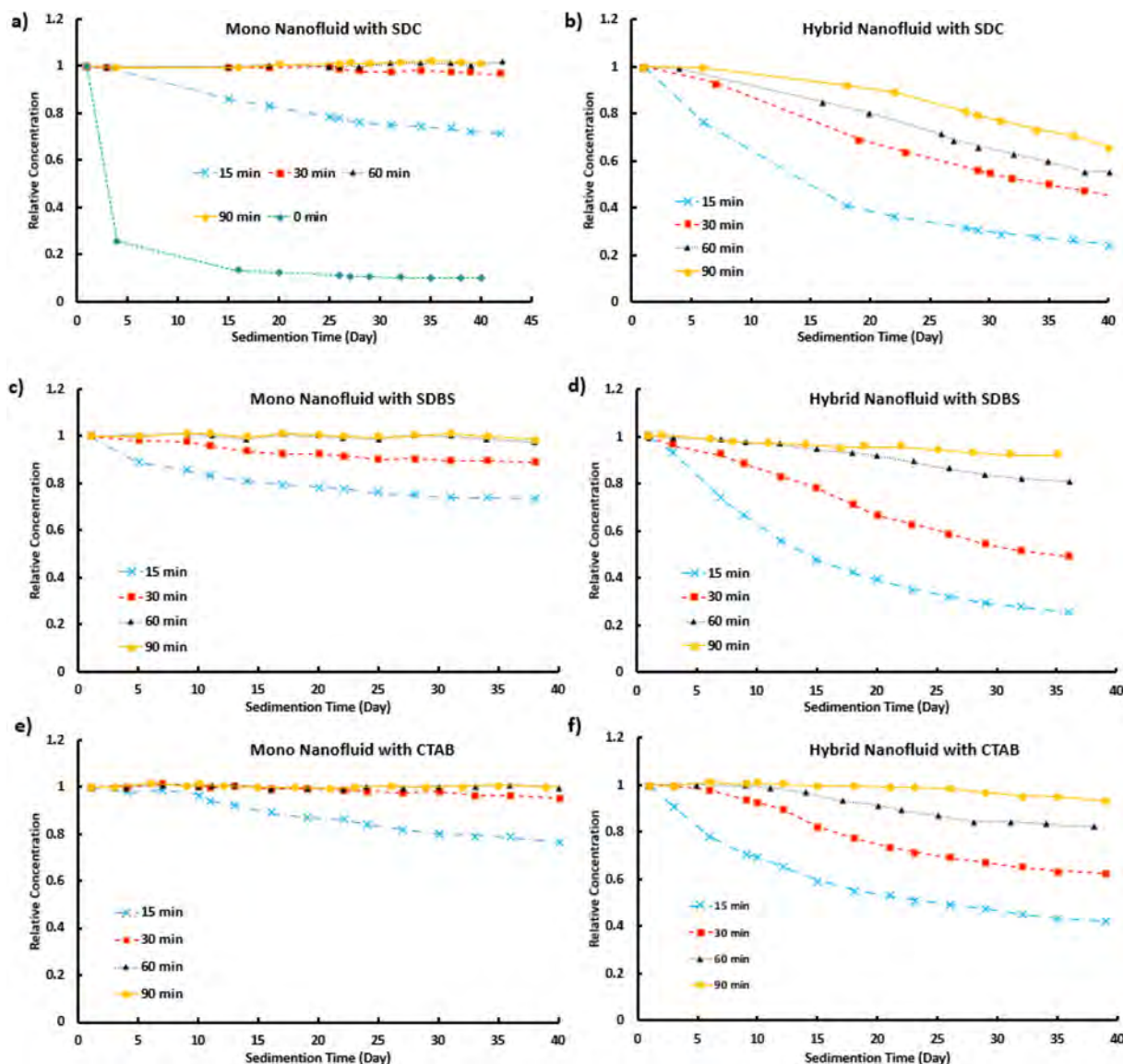


Fig. 8. Relative concentration of nanofluids with sedimentation time.

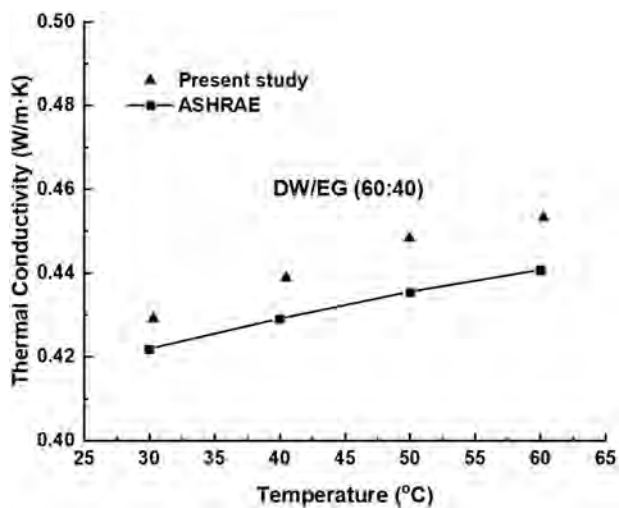


Fig. 9. Validation of experimental data using ASHRAE.

weightage concentration is linearly proportional to absorbance. To validate the experimental procedure, samples with different concentrations were diluted in the ratio of 1:10 to allow sufficient light source transmission and noise reduction on spectrum.

$$A = \epsilon cl = \log \frac{I_0}{I} \tag{1}$$

As can be seen in Fig. 7a, the peak absorbance values of COOH-GnP-SDC nanofluid with four different concentrations were located around a wavelength of 290 nm. Using respective absorbance values from each concentration, a linear relationship between absorbance and concentration of colloids was obtained, which obeyed the Beer-Lambert law.

In this section, only nanofluids with more than ± 30 mV were selected for long term stability inspection. It should be noted that all samples were fixed at 0.1 wt% concentration. Relative concentration (C/C₀) was used to illustrate the behaviour of sedimentation, in which a perfect condition is 1 and a decreased value indicates agglomeration of nanoparticles, followed by sedimentation. Fig. 8 shows the stability of nanofluids with different surfactants up to 40 days of spectroscopy inspection; whereas Table 2 shows respective absorbance drops for each sample at 35th day. Longer ultrasonication time resulted in better

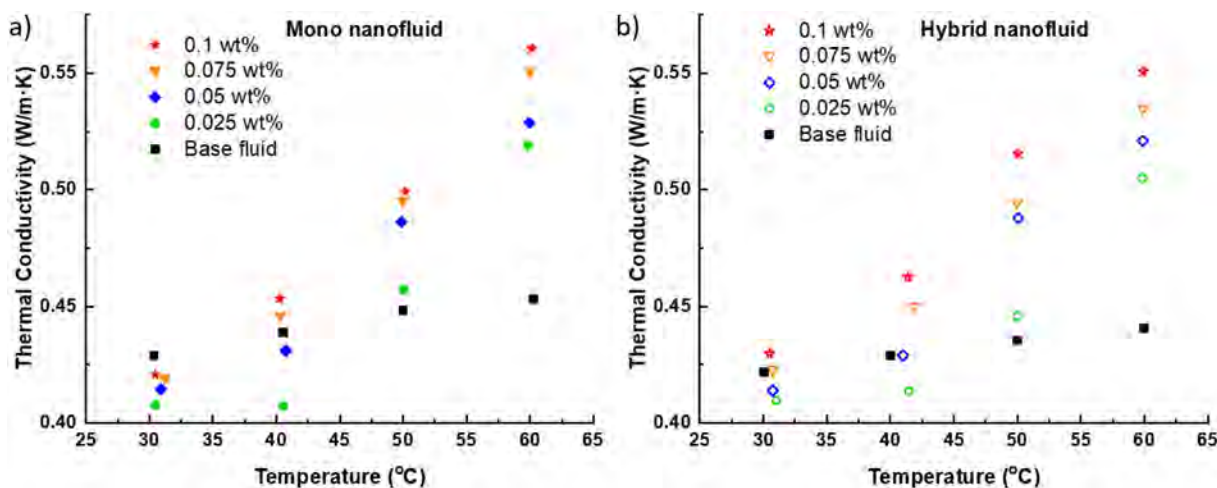


Fig. 10. Thermal conductivity of nanofluids.

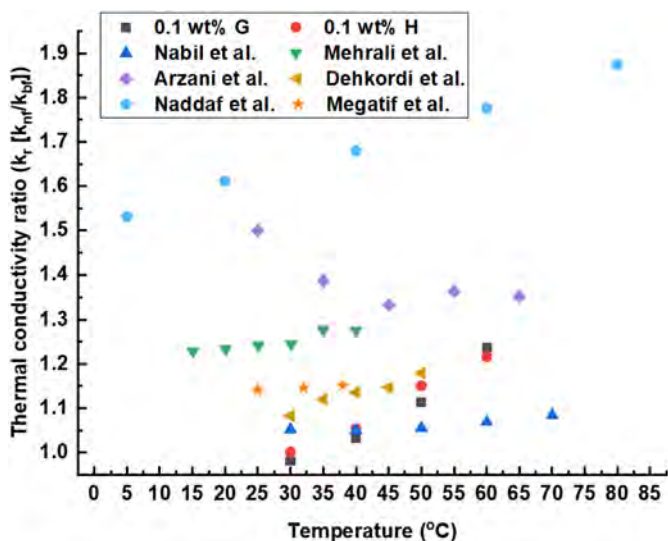


Fig. 11. Comparison with past studies.

stability and Fig. 8a shows that the sample with 0 min of ultrasonication process had poor stability even when SDC was added. All three surfactants showed excellent enhancement of stability in mono nanofluid;

however only SDBS and CTAB were able to prevent more sedimentation in hybrid nanofluid with 90 min of ultrasonication.

3.3. Thermophysical properties

Based on high stability shown on zeta potential and UV-vis spectroscopy analyses, nanofluids with CTAB were chosen for thermal conductivity and viscosity measurement.

3.3.1. Thermal conductivity

Fig. 9 shows the comparison of experimental data with ASHRAE [34], where the average and maximum deviations for thermal conductivity measurement were 2.57% and 3.12%, respectively. From Fig. 10, it can be seen that the thermal conductivity of all samples increased with temperature and concentration. There were various theories or mechanisms explained on the anomalous thermal conductivity behaviour results from different nanoparticles used in past studies. The enhancement in nanofluid thermal conductivity may be due to several factors:

1. Collision of suspended nanoparticles with molecules in base fluid, which is called the Brownian motion. This phenomenon is intensified with the increment of working temperature and concentration of nanoparticles, which lead to higher kinetic energy of nanoparticles and increased rate of collision. In the end, the

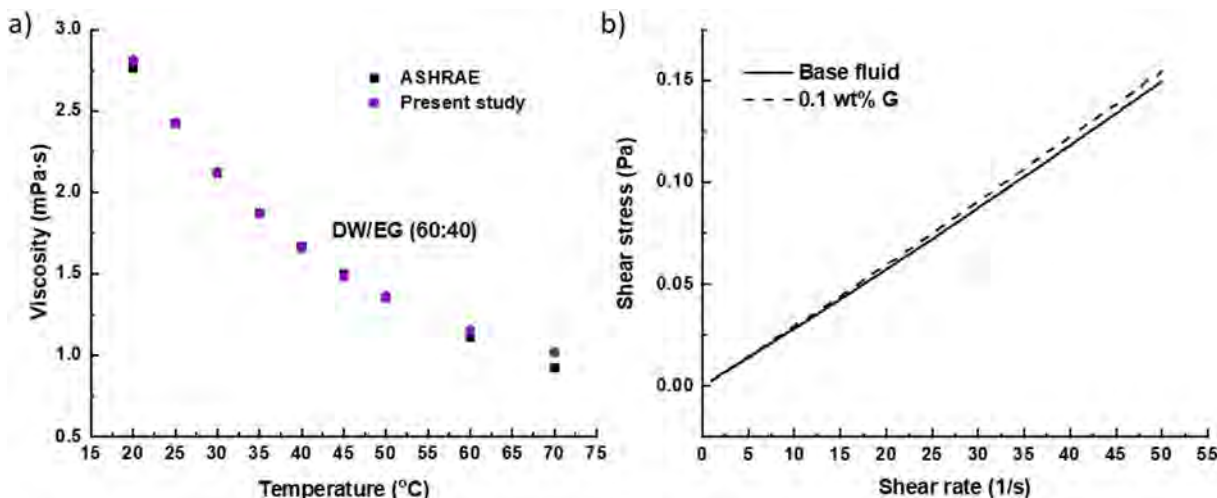


Fig. 12. a) Validation of experimental data using ASHRAE b) Shear stress versus shear rate at 20 °C.

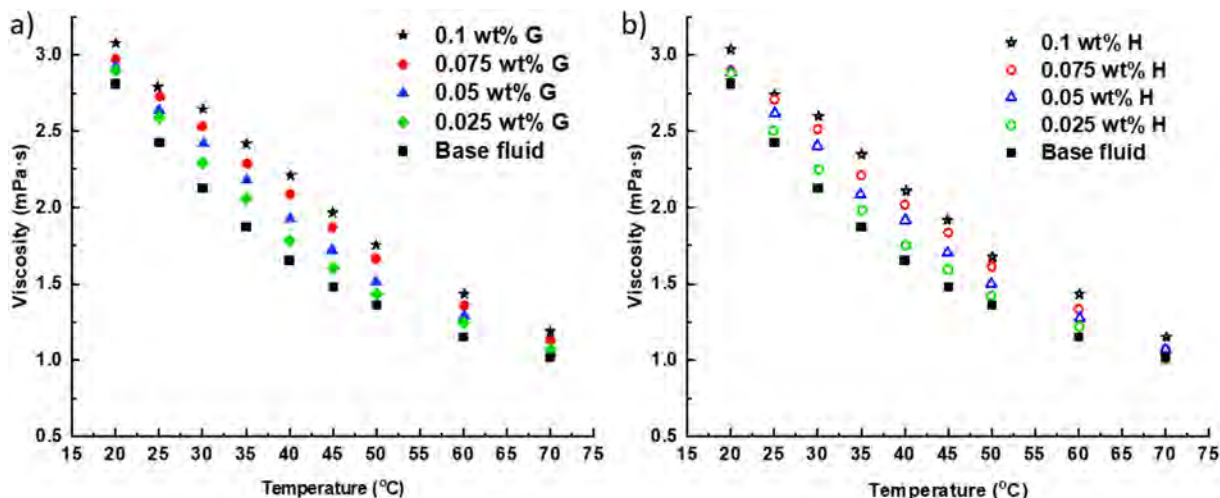


Fig. 13. Viscosity of nanofluids.

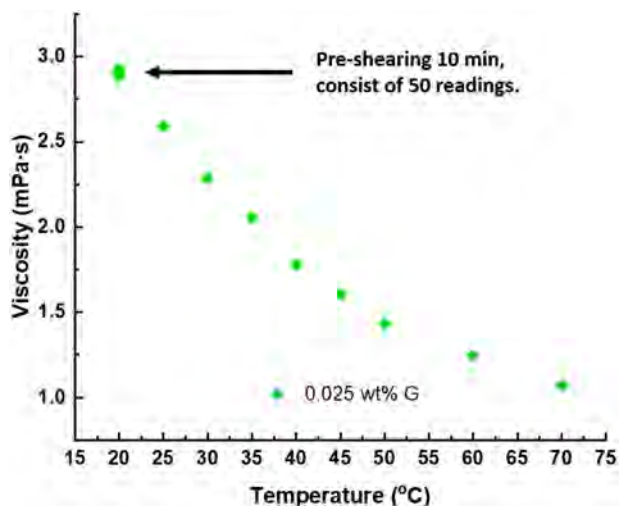


Fig. 14. Pre-shearing of nanofluid.

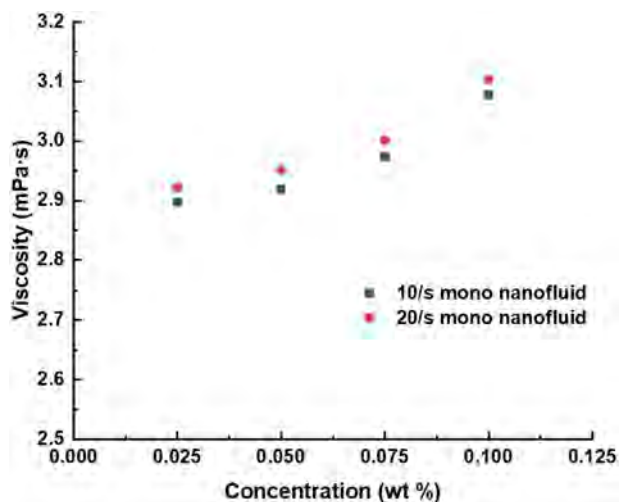


Fig. 15. Viscosity at different shear rates (at 20 °C).

increased rate of heat exchange between nanoparticles and base fluid molecules results in higher thermal conductivity of the suspension.

2. Yu and Choi [35] proposed that the increment of nanofluid thermal

conductivity may occur due to the presence of nanolayer between nanoparticles and bulk fluid, whereby high thermal conducting layered structures are formed when liquid molecules are close to solid particles surface. This phenomenon is only valid for nanoparticles with a diameter of < 10 nm and near-spherical shape.

3. Particles with a high aspect ratio such as carbon nanotubes (CNTs) and GnPs exhibit high diffusive heat conductivity and this behaviour was reported as a dominant factor for increased thermal conductivity in hybrid nanofluids [36].
4. The increased concentration of nanoparticles indicates decreasing particle-to-particle distance. The closer gap between particles allows increased frequency of lattice vibration and increased thermal conductivity. This mechanism is known as the percolation effect [37].
5. It was suggested by many past researchers that the high thermal conductivity of nanoparticles leads to heat transfer enhancement when compared to base fluid. Nevertheless, previous studies [2,3,38,39] showed that hybrid nanofluid exhibited lower thermal conductivity and some believed that nanoparticles with low thermal conductivity tend to increase thermal resistance instead of thermal conductance when mixed with high thermal conductivity nanoparticles. From a recent numerical work [40], it was found that thermal conductivity obtained using some theoretical and numerical models was lower than their work due to overlook of some important factors which include shape and size of nanoparticles.

In the present study, there was no significant difference between thermal conductivity of mono and hybrid nanofluids. As shown in Fig. 10, all nanofluids showed lower thermal conductivity than base fluid at 30 °C. Thermal conductivity of all nanofluids were then improved by increasing temperature and concentration. The dominant factor for increased thermal conductivity for both nanofluids was mainly due to the intrinsic high thermal conductivity of COOH-GnPs, Brownian motion and followed by concentration of nanoparticles. The maximum thermal conductivity enhancement was observed at 60 °C, where 0.1 wt% mono nanofluid and hybrid nanofluid showed 23.74% and 21.59% of increment, respectively, when compared to base fluid. At the same temperature, the addition of 0.025 wt% hybrid nanoparticles showed less enhancement (11.46%) on base fluid, while mono nanofluid was 3.09% relatively higher than hybrid. At higher concentration (0.1 wt% and 0.075 wt%), hybrid nanofluid showed higher thermal conductivity than mono nanofluid at all temperature except 60 °C (1.73% lower). Surprisingly, both mono and hybrid nanofluids exhibit similar heat transfer behavior at 0.05 wt% concentration. For 0.025 wt% nanofluids, minor deterioration was found at 50 and 60 °C

Table 1
Surfactants used in this study.

Surfactant	Commercial source	Remark
Polyvinylpyrrolidone (PVP)	Merck	Non-ionic
Triton X-100	Merck	Non-ionic, pH 6–8
Dodecyl sulfate sodium salt (SDS)	Merck	Anionic, 288.37 g/mol
Sodium deoxycholate (SDC)	J&K	Anionic, 98% purity
Sodium dodecylbenzenesulfonate (SDBS)	Sigma Aldrich	Anionic, technical grade, 348.48 g/mol
Hexadecyltrimethylammonium bromide (CTAB)	Sigma Aldrich	Cationic, > 98% purity, 364.45 g/mol

Table 2
Sedimentation amount of tested samples.

Sonication time	Surfactant					
	SDC		CTAB		SDBS	
	Absorbance drop at 35th day (%)					
	Mono	Hybrid	Mono	Hybrid	Mono	Hybrid
15 min	25.82	72.41	21.44	56.84	26.10	74.58
30 min	1.88	50.01	3.570	36.54	10.71	50.64
60 min	Negligible	40.36	Negligible	16.38	Negligible	19.01
90 min	Negligible	26.47	Negligible	5.124	Negligible	7.58

when hybrid type was compared to mono type. The authors believed that the insignificant enhancement of hybridization between TiO₂ and COOH-GnP nanoparticles might be due to the lack of synergistic effect based on several past studies: mixing different nanoparticles with similar size and shape [41], inappropriate mixing ratio [23,42], mixing nanoparticles with a huge gap of thermal conductivity [2], and inefficient amount or type of surfactant [22,43]. A similar past study showed that 0.1 wt% of multi-walled carbon nanotubes (MWCNT) nanofluid had higher thermal conductivity than both MWCNT-TiO₂ hybrid nanofluid and base fluid [44]. In addition, some authors obtained a similar trend as the present study during their thermal conductivity measurement [2,3,39] and heat transfer applications [38,41].

On the other hand, nanofluids with similar nanoparticles/base fluid used in past studies were compared with the present study in terms of thermal conductivity ratio and some details are tabulated in Table 3 below. Based on Fig. 11, it can be inferred that the addition of surfactants might be the main cause limiting thermal conductivity increment.

3.3.2. Viscosity

Measured viscosity of base fluid was compared with ASHRAE and the average deviation was found to be 1.68%, as presented in Fig. 12a. On the other hand, Fig. 12b shows a linear relation between the shear stress and shear rate of base fluid and 0.1 wt% G at 20 °C. Thus, the tested base fluid and nanofluids behaved as Newtonian fluids. The higher shear stress of nanofluid in comparison to base fluid at the same shear rate indicated higher viscosity and the effect was clearer at a higher shear rate. This is because greater torque is required by the equipment spindle for stirring during measurement. As a result, the

Table 3
Details of nanofluids used in past studies.

Author	Nanoparticles	Base fluid	Nanoparticles concentration	Surfactant
Present study	COOH-GnP	DW/EG (60:40)	0.1 wt%	CTAB
Present study	COOH-GnP + TiO ₂ (50:50)	DW/EG (60:40)	0.1 wt%	CTAB
Megatif et al. [44]	TiO ₂ + MWCNT	Water	0.1 wt%	SDBS
Nabil et al. [45]	TiO ₂ + SiO ₂	W/EG (60:40)	1 vol%	–
Mehrali et al. [46]	GnP (750 m ² /g)	DW	0.1 wt%	–
Arzani et al. [47]	EG functionalised GnP	W/EG (40:60)	0.1 wt%	–
Dehkordi et al. [48]	COOH-SWCNT	W/EG (50:50)	0.125 vol%	–
Naddaf et al. [11]	GnP + MWCNT (50:50)	Diesel oil	0.1 wt%	Oleic acid

viscosity of suspension increased when the concentration of dispersed nanoparticles increased, as shown in Fig. 13. A similar trend of viscosity behaviour was observed in most past studies where the viscosity drop gradually decreased with increasing temperature. This phenomenon is due to the fact that high temperature weakened intermolecular and interparticle interactions [49]. In the present study, the viscosity of mono nanofluid was found to be higher than hybrid nanofluid and base fluid. At 40 °C, 0.1 wt% G showed 32.54% of maximum viscosity increment, while 0.1 wt% H showed 26.41% when compared to DW/EG.

Apart from that, past studies [46] mentioned the pseudoplastic behaviour of samples at the starting of measurement. Initially, the spindle required higher torque to rotate against friction force due to nearly-static fluid molecules and nanoparticles in suspension. When those molecules and nanoparticles started to align themselves in the rotating direction, friction and viscosity would decrease. Thus, pre-shearing was performed for all samples in the present study to avoid any possible inaccuracy. Before starting the measurement, the pre-shear option was selected in the software with the setting of shear rate from 50/s to 10/s fixing at 20 °C. Fig. 14 shows a small change of viscosity result throughout the pre-shearing of 10 min at 20 °C.

However, the flow behaviour of samples over 50/s was not reported. There were several attempts performed and it was observed that a shear rate over 50/s caused gradual increment in viscosity. The trend was most probably due to the turbulence vortex created by the high flowing rate in the cylinder container, although it is supposedly suitable for low viscosity liquid measurement. Turbulence vortex was inclined to increase the viscosity of flowing fluid and it caused inaccuracy of results in the present study. Thus, the authors tested two low shear rates (10/s and 20/s) at 20 °C and determined the effect on viscosity of COOH-GnP nanofluid at different concentrations. As can be seen clearly in Fig. 15, the viscosity results from two different shear rates were close to each other. This suggested that the low shear rate in the concentric cylinder measuring system was able to provide accurate and consistent results, which were similar to most authors who obtained consistent results using cone plate at a high shear rate.

4. Conclusion

The stability, thermal conductivity, and viscosity of (COOH-GnP)-TiO₂ nanofluids were determined from 30 °C to 70 °C with four different concentrations (0.025, 0.05, 0.075, and 0.1 wt%). Ultrasonication of 90 min was sufficient to produce highly stable hybrid nanofluids with

the addition of CTAB or SDBS. Based on multiple stability analyses, CTAB was found to be the best surfactant to stabilise this hybrid nanofluid. Thermal conductivity of nanofluids increased with both temperature and concentration of nanoparticles, with the most significant enhancement (23.74%) observed at 60 °C and 0.1 wt%. Hybrid nanofluid showed higher thermal conductivity than COOH-GnP nanofluid at all concentration with lower temperature (30 to 50 °C), which means mono nanofluid surpass hybrid nanofluid at 60 °C (all concentration). High thermal conductivity of COOH-GnP was found to be the dominant factor to enhance thermal behaviour of both mono and hybrid nanofluids. Shear stress was increased when nanoparticles were added into the base fluid. Viscosity of both mono and hybrid nanofluids showed about 6% of difference at 0.1 wt% concentration and 40 °C working temperature. The enhanced thermal property by adding nanoparticles suggested this novel hybrid nanofluid could be used as an alternate heat transfer medium.

Acknowledgement

The authors wish to thank Universiti Teknologi Malaysia for supporting this research activity under the Takasago grant (R.K130000.7343.4B314). Additionally, R. Saidur would like to acknowledge the financial support provided by Sunway University through the project no. STR-RCTR-RCNMET-001-2019.

References

- [1] S.U. Choi, J.A. Eastman, Enhancing Thermal Conductivity of Fluids with Nanoparticles, Argonne National Lab, IL (United States), 1995.
- [2] S. Jana, A. Salehi-Khojin, W.-H. Zhong, Enhancement of fluid thermal conductivity by the addition of single and hybrid nano-additives, *Thermochim. Acta* 462 (1) (2007) 45–55.
- [3] H.W. Xian, N.A.C. Sidik, S.R. Aid, T.L. Ken, Y. Asako, Review on preparation techniques, properties and performance of hybrid nanofluid in recent engineering applications, *J. Adv. Res. Fluid Mech. Therm. Sci.* 45 (1) (2018) 1–13.
- [4] S.S.J. Aravind, S. Ramaprabhu, Graphene-multiwalled carbon nanotube-based nanofluids for improved heat dissipation, *RSC Adv.* 3 (13) (2013) 4199–4206.
- [5] S. Aman, S.M. Zokri, Z. Ismail, M.Z. Salleh, I. Khan, Effect of MHD and porosity on exact solutions and flow of a hybrid cation-nanofluid, *J. Adv. Res. Fluid Mech. Therm. Sci.* 44 (1) (2018) 131–139.
- [6] R.R. Sahoo, P. Ghosh, J. Sarkar, Performance analysis of a louvered fin automotive radiator using hybrid nanofluid as coolant, *Heat Transf. Asian Res.* 46 (7) (2017) 978–995.
- [7] C. Selvam, D. Mohan Lal, S. Harish, Thermal conductivity and specific heat capacity of water–ethylene glycol mixture-based nanofluids with graphene nanoplatelets, *J. Therm. Anal. Calorim.* 129 (2) (2017) 947–955.
- [8] A. Hilo, A.R.A. Talib, S.R. Nfawa, ... M.F.A. Hamid, M.I. Nadiir Bheekhun, Heat transfer and thermal conductivity enhancement using graphene nanofluid: A review, *J. Adv. Res. Fluid Mech. Therm. Sci.* 55 (1) (2019) 74–87.
- [9] H.K. Arzani, et al., Heat transfer performance of water-based tetrahydrofurfuryl polyethylene glycol-treated graphene nanoplatelet nanofluids, *RSC Adv.* 6 (70) (2016) 65654–65669.
- [10] M.M. Sarafraz, et al., Fluid and heat transfer characteristics of aqueous graphene nanoplatelet (GNP) nanofluid in a microchannel, *Int. Commun. Heat Mass Transf.* 107 (2019) 24–33.
- [11] A. Naddaf, S. Zeinali Heris, Experimental study on thermal conductivity and electrical conductivity of diesel oil-based nanofluids of graphene nanoplatelets and carbon nanotubes, *Int. Commun. Heat Mass Transf.* 95 (2018) 116–122.
- [12] P. Van Trinh, et al., Experimental study on the thermal conductivity of ethylene glycol-based nanofluid containing gr-CNT hybrid material, *J. Mol. Liq.* 269 (2018) 344–353.
- [13] W. Zheng, B. Shen, W. Zhai, Surface functionalization of graphene with polymers for enhanced properties, *New Progress on Graphene Research*, IntechOpen, 2013.
- [14] H. Yarmand, et al., Graphene nanoplatelets–silver hybrid nanofluids for enhanced heat transfer, *Energy Convers. Manag.* 100 (2015) 419–428.
- [15] S.S. Shazali, et al., Evaluation on stability and thermophysical performances of covalently functionalized graphene nanoplatelets with xylitol and citric acid, *Mater. Chem. Phys.* 212 (2018) 363–371.
- [16] M. Ioniță, et al., Graphene and functionalized graphene: extraordinary prospects for nanobiocomposite materials, *Compos. Part B* 121 (2017) 34–57.
- [17] Z. Wang, et al., Experimental comparative evaluation of a graphene nanofluid coolant in miniature plate heat exchanger, *Int. J. Therm. Sci.* 130 (2018) 148–156.
- [18] J.P. Vallejo, et al., Functionalized graphene nanoplatelet nanofluids based on a commercial industrial antifreeze for the thermal performance enhancement of wind turbines, *Appl. Therm. Eng.* 152 (2019) 113–125.
- [19] E. Sani, et al., Functionalized graphene nanoplatelet-nanofluids for solar thermal collectors, *Sol. Energy Mater. Sol. Cells* 185 (2018) 205–209.
- [20] A. Akbari, et al., Thermo-physical and stability properties of raw and functionalization of graphene nanoplatelets-based aqueous nanofluids, *J. Dispers. Sci. Technol.* 40 (1) (2019) 17–24.
- [21] A.H.A. Al-Waeli, et al., Evaluation and analysis of nanofluid and surfactant impact on photovoltaic-thermal systems, *Case Stud. Therm. Eng.* 13 (2019) 100392.
- [22] K.Y. Leong, et al., Thermal conductivity of an ethylene glycol/water-based nanofluid with copper-titanium dioxide nanoparticles: an experimental approach, *Int. Commun. Heat Mass Transf.* 90 (2018) 23–28.
- [23] F.R. Siddiqui, et al., On trade-off for dispersion stability and thermal transport of Cu-Al₂O₃ hybrid nanofluid for various mixing ratios, *Int. J. Heat Mass Transf.* 132 (2019) 1200–1216.
- [24] A.I. El-Seesy, H. Hassan, Investigation of the effect of adding graphene oxide, graphene nanoplatelet, and multiwalled carbon nanotube additives with n-butanol-Jatropha methyl ester on a diesel engine performance, *Renew. Energy* 132 (2019) 558–574.
- [25] K.Y. Leong, et al., Synthesis and thermal conductivity characteristic of hybrid nanofluids – a review, *Renew. Sust. Energ. Rev.* 75 (2017) 868–878.
- [26] H. Yarmand, et al., Study of synthesis, stability and thermo-physical properties of graphene nanoplatelet/platinum hybrid nanofluid, *Int. Commun. Heat Mass Transf.* 77 (2016) 15–21.
- [27] A. Giampiccolo, et al., Sol gel graphene/TiO₂ nanoparticles for the photocatalytic-assisted sensing and abatement of NO₂, *Appl. Catal. B Environ.* 243 (2019) 183–194.
- [28] U.A. Kanta, et al., Preparations, characterizations, and a comparative study on photovoltaic performance of two different types of graphene/TiO₂ nanocomposites photoelectrodes, *J. Nanomater.* 2017 (2017).
- [29] M. Nurdin, et al., Synthesis and electrochemical performance of graphene-TiO₂-carbon paste nanocomposites electrode in phenol detection, *J. Phys. Chem. Solids* 131 (2019) 104–110.
- [30] D. Dhinesh Kumar, A. Valan Arasu, A comprehensive review of preparation, characterization, properties and stability of hybrid nanofluids, *Renew. Sust. Energ. Rev.* 81 (2018) 1669–1689.
- [31] F. Yu, et al., Dispersion stability of thermal nanofluids, *Prog. Nat. Sci. Mater. Int.* 27 (5) (2017) 531–542.
- [32] N. Ahammed, L.G. Asirvatham, S. Wongwises, Effect of volume concentration and temperature on viscosity and surface tension of graphene–water nanofluid for heat transfer applications, *J. Therm. Anal. Calorim.* 123 (2) (2016) 1399–1409.
- [33] L.J. Felicia, J.C. Johnson, J. Philip, Effect of surfactant on the size, zeta potential and rheology of alumina nanofluids, *J. Nanofluid.* 3 (4) (2014) 328–335.
- [34] R.H. Howell, Principles of Heating Ventilating and Air Conditioning: A Textbook with Design Data Based on the 2017, *Ashrae Handbook Fundamentals*, ASHRAE, 2017.
- [35] W. Yu, S.U.S. Choi, The role of interfacial layers in the enhanced thermal conductivity of nanofluids: a renovated Maxwell model, *J. Nanopart. Res.* 5 (1) (2003) 167–171.
- [36] Z.H. Han, et al., Application of hybrid sphere/carbon nanotube particles in nanofluids, *Nanotechnology* 18 (10) (2007).
- [37] T.T. Baby, R. Sundara, Synthesis and transport properties of metal oxide decorated graphene dispersed nanofluids, *J. Phys. Chem. C* 115 (17) (2011) 8527–8533.
- [38] N. Ahammed, L.G. Asirvatham, S. Wongwises, Entropy generation analysis of graphene–alumina hybrid nanofluid in multiport minichannel heat exchanger coupled with thermoelectric cooler, *Int. J. Heat Mass Transf.* 103 (2016) 1084–1097.
- [39] G.M. Moldoveanu, et al., Experimental study on thermal conductivity of stabilized Al₂O₃ and SiO₂ nanofluids and their hybrid, *Int. J. Heat Mass Transf.* 127 (2018) 450–457.
- [40] Ç. Yildiz, M. Arıcı, H. Karabay, Comparison of a theoretical and experimental thermal conductivity model on the heat transfer performance of Al₂O₃-SiO₂/water hybrid-nanofluid, *Int. J. Heat Mass Transf.* 140 (2019) 598–605.
- [41] V. Kumar, J. Sarkar, Numerical and experimental investigations on heat transfer and pressure drop characteristics of Al₂O₃-TiO₂ hybrid nanofluid in minichannel heat sink with different mixture ratio, *Powder Technol.* 345 (2019) 717–727.
- [42] K.A. Hamid, et al., Heat transfer augmentation of mixture ratio TiO₂ to SiO₂ in hybrid nanofluid, *Aust. J. Mech. Eng. SI* 4 (3) (2017) 51–63.
- [43] B. White, et al., Zeta-potential measurements of surfactant-wrapped individual single-walled carbon nanotubes, *J. Phys. Chem. C* 111 (37) (2007) 13684–13690.
- [44] L. Megatiff, et al., Investigation of laminar convective heat transfer of a novel TiO₂-carbon nanotube hybrid water-based nanofluid, *Experiment. Heat Transf.* 29 (1) (2016) 124–138.
- [45] M.F. Nabil, et al., An experimental study on the thermal conductivity and dynamic viscosity of TiO₂-SiO₂ nanofluids in water: ethylene glycol mixture, *Int. Commun. Heat Mass Transf.* 86 (2017) 181–189.
- [46] M. Mehrali, et al., Investigation of thermal conductivity and rheological properties of nanofluids containing graphene nanoplatelets, *Nanoscale Res. Lett.* 9 (1) (2014).
- [47] H. Khajeh Arzani, et al., Toward improved heat transfer performance of annular heat exchangers with water/ethylene glycol-based nanofluids containing graphene nanoplatelets, *J. Therm. Anal. Calorim.* 126 (3) (2016) 1427–1436.
- [48] R. Adhami Dehkordi, M. Hemmat Esfe, M. Afrand, Effects of functionalized single walled carbon nanotubes on thermal performance of antifreeze: an experimental study on thermal conductivity, *Appl. Therm. Eng.* 120 (2017) 358–366.
- [49] M. Afrand, D. Toghraie, B. Ruhani, Effects of temperature and nanoparticles concentration on rheological behavior of Fe₃O₄-Ag/EG hybrid nanofluid: an experimental study, *Exp. Thermal Fluid Sci.* 77 (2016) 38–44.